18th International Conference on Structural Mechanics in Reactor Technology (SMiRT 18)
Beijing, China, August 7-12, 2005
SMiRT 18-G11-11

EFFECTS OF LOADING FACTORS ON ENVIRONMENTAL FATIGUE BEHAVIOR OF LOW-ALLOY PRESSURE VESSEL STEEL IN SIMULATED BWR WATER

X. Q. Wu, E. H. Han, W. Ke
Environmental Corrosion Center, Institute of Metal Research, Chinese Academy of Sciences, 62 Wencui Road, Shenyang 110016, P.R. China
Y. Katada
National Institute for Materials Science, 1-2-1 Sengen, Tsukuba, Ibaraki 305-0047, Japan

Abstract
Low cycle fatigue resistance of low-alloy pressure vessel steels was investigated in simulated boiling water reactor (BWR) water. Much attention was paid to the effects of loading factors on fatigue life and environmentally assisted cracking (EAC) behavior, in which strain rate, strain waveform and strain amplitude were considered. The fatigue resistance and EAC behavior of the steels in simulated BWR water were found to be closely dependent on the strain rate, strain waveform and strain amplitude applied. The above environmental fatigue behavior may be attributed to loading-factor-induced change in dominant EAC processes. Related EAC mechanisms are also discussed.
Keywords: pressure vessel steels, low cycle fatigue, BWR, EAC

1. Introduction
In connection with the light water reactor (LWR) environments various environmentally assisted cracking (EAC) issues should be cautiously considered for the reactor pressure vessel (PRV) and piping system for purposes of safety managements and remaining life assessment of nuclear power plants, among which corrosion fatigue is of great significance [1]. The higher safety requirements force the development of qualified materials and new strict design criteria to ensure the structural integrity in nuclear power plants throughout their design lives (typical 40 years for a boiling water reactor (BWR)). To meet these requirements, testing of LWR structural materials under service loading and environmental conditions, data generation, and clarification of related EAC processes are a necessary and long-term work. The present attention was mainly paid to the influence of loading factors such as strain rate, strain waveform and strain amplitude on low cycle fatigue (LCF) resistance and EAC behavior of low-alloy RPV steels in high temperature water.

2. Experimental
Three hot-rolled A533B RPV steel plates and a forged A508 Cl.3 steel were used for the present study, whose chemical compositions and heat-treatments are shown in Table 1. The

as-received microstructure of all materials is upper bainite. Cylindrical LCF specimens with 8 mm gauge diameter and 16 mm gauge length were machined along the rolling or forged direction. The equipments for LCF tests comprised a MTS fatigue testing machine of 100 kN in dynamic load, an austenitic stainless steel autoclave of 6 liter per hour in capacity and a water loop with 30 liter per hour flow rate. Fatigue tests were performed in an axial control mode with fully reversed triangular waveform. A simulated BWR water chemistry, *i.e.*, 100 ppb dissolved oxygen concentration (DO), 6.2 to 6.5 pH, and <0.2 $\mu S \cdot cm^{-1}$ conductivity, was used in the present study. The test temperature and pressure were 561 K and 8.0 MPa. Fatigue life, N_{25}, was defined as the number of cycles for tensile stress to drop 25 % from its peak value. Some tested specimens were broken apart in liquid nitrogen. A scanning electron microscope was employed to inspect the cracking/fractographic features.

Table 1 Chemical compositions (wt.%) and heat-treatments of low-alloy RPV steels used.

Steels	C	Si	Mn	S	P	Ni	Cr	Mo	Cu	Al	Fe
A533B (L-S)*	**0.17**	**0.25**	**1.39**	**0.013**	**0.003**	**0.59**	**0.004**	**0.46**	**0.005**	**0.026**	**Bal.**
A533B (M-S)*	**0.17**	**0.24**	**1.38**	**0.025**	**0.003**	**0.60**	**0.004**	**0.47**	**0.005**	**0.024**	**Bal.**
A533B (LL-S)*	**0.19**	**0.24**	**1.28**	**0.007**	**0.008**	**0.64**	**0.19**	**0.45**	**0.04**	**–**	**Bal.**
A508 Cl.3**	**0.21**	**0.25**	**1.24**	**0.002**	**0.007**	**0.88**	**0.21**	**0.47**	**0.03**	**0.008**	**Bal.**

*: 1173 K × 3 h water quenching, 933 K × 3 h air cooling, then 873 K × 25 h to relieve stress.
**: 1153 K × 7 h water quenching, 928 K × 9 h air cooling.

3.Results and Discussion

3.1 Effects of strain rate

Fig. 1a shows the *S-N* curves for low-alloy RPV steel A533B (L-S) in simulated BWR water. The data obtained in 561 K air are also included for the comparison. It is clear that the fatigue resistance of the steel in the moderate and high strain ranges degraded obviously due to environmental effects. Decreasing strain rate led to distinct degradation of fatigue resistance of the steel in high temperature water. Fig. 1b shows the dependence of fatigue life on strain rate in simulated BWR water under different strain range conditions. At the strain rate above 0.001 $\%s^{-1}$, the fatigue life decreased almost linearly with a decrease in strain rate on a log-log plot, indicating strain-rate dependent environmental effects. However, the environmental

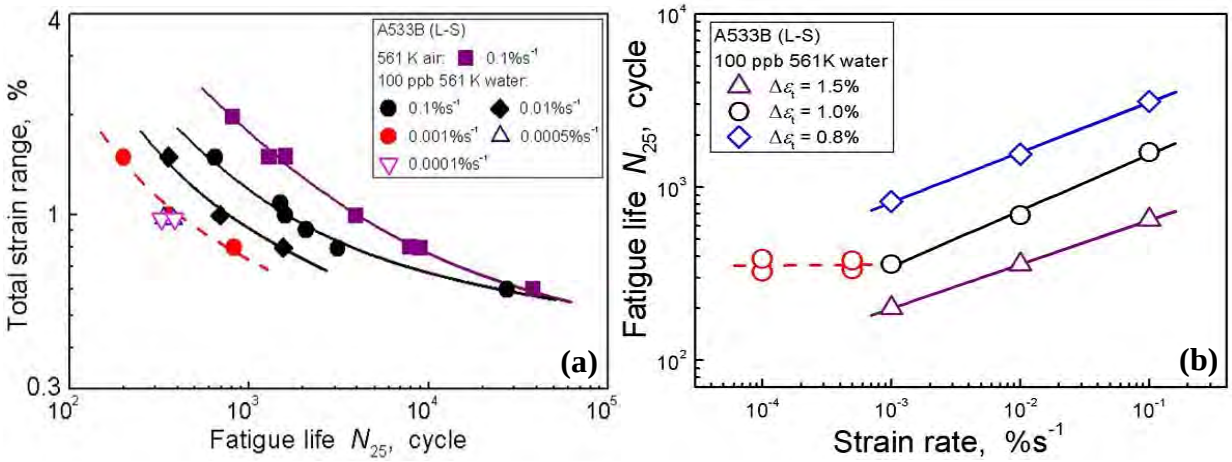

Fig. 1 S-N curves (a) and dependence of fatigue life on strain rate (b) for A533B (L-S) steel in simulated BWR water

effects tended to become saturated at the strain rate below 0.001 $\%s^{-1}$ as shown in Fig. 1b, which was in good agreement with Chopra and Shack's results [2].

Fig. 2 is the macro-morphologies of fatigue cracks on specimen surfaces. In 561 K air, fatigue crack was tortuous, and was about 45^{o} inclined to the loading axis regardless of strain rate (Fig. 2a). In 561 K water, crack morphology was dependent on strain rate. At high strain rate (0.1 $\%s^{-1}$), fatigue crack was similar to that in air, but showed obvious macro-branching (Fig. 2b). With a decrease in strain rate, fatigue crack tended to become entirely straight and normal to the loading axis (Fig. 2c and 2d).

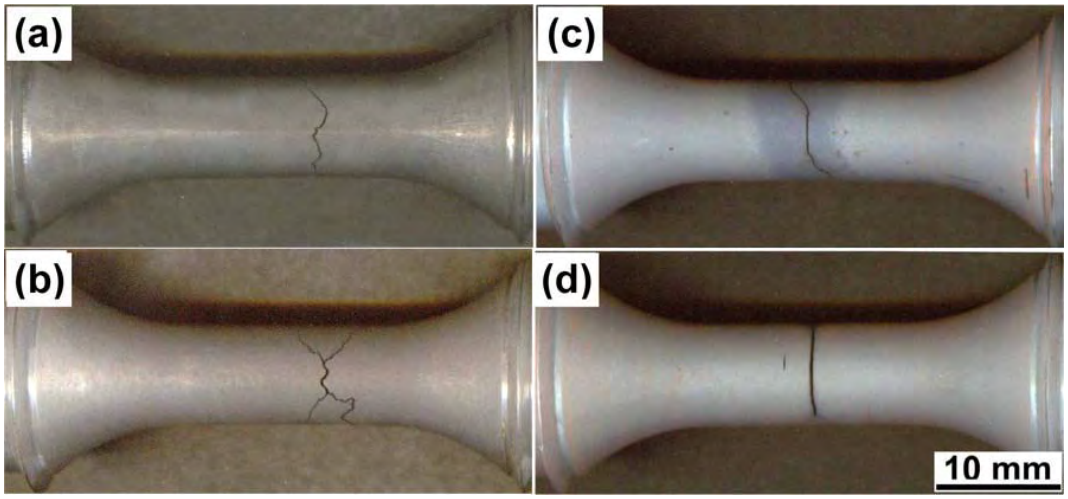

Fig. 2 Macro-morphologies of fatigue cracks on specimen surfaces, 0.75 % strain amplitude. (a) 561 K air, 0.1 $\%s^{-1}$ (b) (c) (d) 561 K 100 ppb water, 0.1 $\%s^{-1}$, 0.01 $\%s^{-1}$, 0.001 $\%s^{-1}$ respectively.

Fig. 3 shows typical fracture morphologies. A rough fracture was observed in 561 K air (Fig. 3a) and in 561 K water at high strain rate (Fig. 3c). Despite covered by heavy oxides,

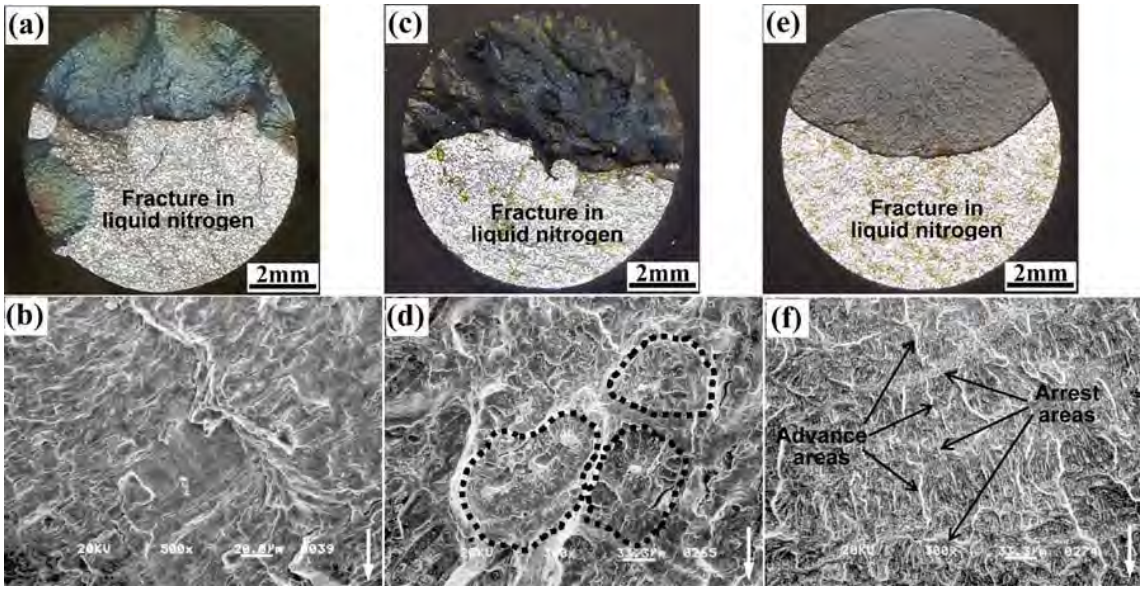

Fig. 3 Fatigue fracture morphologies, 0.5% strain amplitude. (a)(b) 561 K air, 0.1 $\%s^{-1}$ (c)(d) 561 K water, 0.1 $\%s^{-1}$ (e)(f) 561 K water, 0.001 $\%s^{-1}$. (b)(d)(f) are the high magnification of

under high magnification the fracture surface in 561 K air still showed some striation-like

features (Fig. 3b), while fan-like patterns (marked in Fig. 3d) were frequently observed around MnS inclusions on the fracture surface in 561 K water at high strain rate. At low strain rate, a flat fracture was observed (Fig. 3e), on which slight crack arrest traces rather than fan-like features were found (Fig. 3f).

Two distinguished cracking morphologies were observed in the present study and showed an intimate dependence on strain rate. This strain-rate dependent cracking behavior could be attributed to a change in dominant EAC mechanism. To date, two basic mechanisms, *i.e.*, hydrogen-induced cracking model and film-rupture/slip dissolution model, have been widely proposed and broadly accepted for interpreting the EAC behavior of RPV steels in high temperature water. In the present work, at high strain rate (0.1 $\%s^{-1}$), tortuous cracks with obvious macro-branching (Fig. 2b) were dominant and fan-like patterns (Fig. 3d) were frequently observed on the fracture surfaces. This seemed to suggest hydrogen-induced cracking dominate the EAC process, in agreement with the previous studies [3, 4]. At low strain rate (0.001 $\%s^{-1}$), however, entirely straight cracks (Fig. 2d) were dominant and slight crack arrest traces were observed on the fracture surfaces (Fig. 3f). These cracking features seemed to agree well with the film-rupture/slip-dissolution model, coinciding with the suggestions of Chopra *et al.* [5] and Scully [6].

3.2 Effects of strain waveform

In the present study, six types of strain waveforms, as shown in Fig. 4, were used to investigate the influence of strain waveforms on fatigue resistance of low-alloy RPV steel A533B (M-S) in high temperature water. Fig. 5 shows the *S-N* curves. The applied strain waveforms had obvious effects on the fatigue life of the steel in high temperature water. This can be more clearly seen from the relationship between the fatigue life and the fraction of strain at slow strain rate f_s, as shown in Fig. 6. Increasing the f_s remarkably decreased the fatigue life, in particular when $f_s < 0.5$, regardless of the applied strain amplitude.

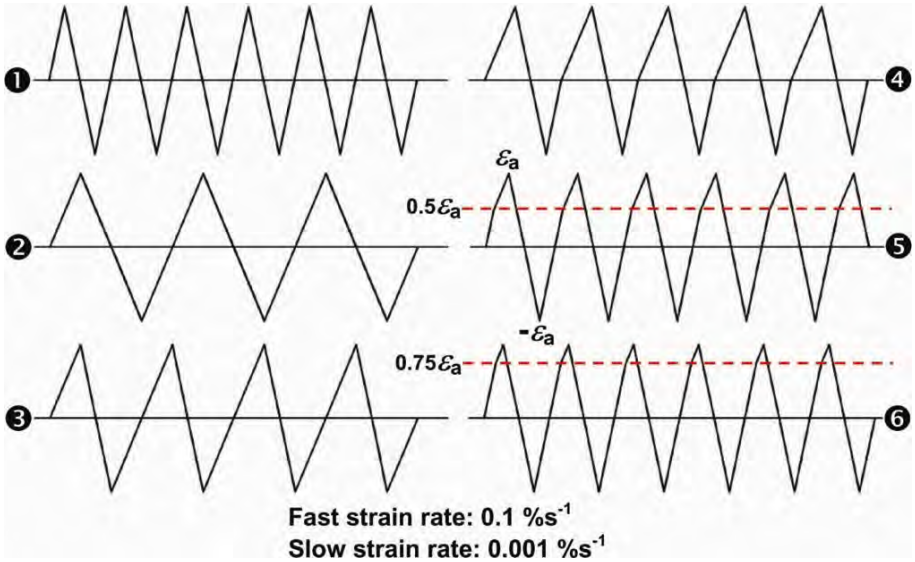

Fig. 4 Strain waveforms used in the present study.

Fig. 7 shows the corresponding fatigue crack morphologies on the specimen surfaces in

high temperature water. Different strain waveforms resulted in much different surface crack morphologies. For the strain waveforms with larger fraction of strain at fast strain rate (0.1 $\%s^{-1}$), the surface cracks developed in a zigzag manner and tended to be inclined to the loading axis (Fig. 7a and 7b). With increase of the fraction of strain at slow strain rate (0.001 $\%s^{-1}$), the surface cracks tended to become entirely straight and completely normal to the loading axis (Fig. 7c to 7e).

The above results can also be rationalized by the strain-rate dependent EAC mechanism as discussed in the previous section.

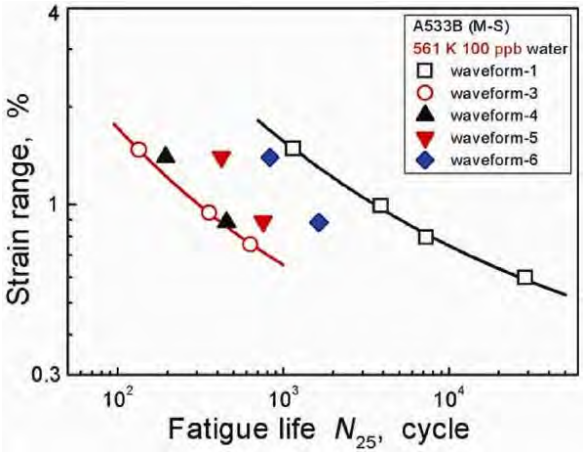

Fig. 5 Effects of strain waveform on S-N curves.

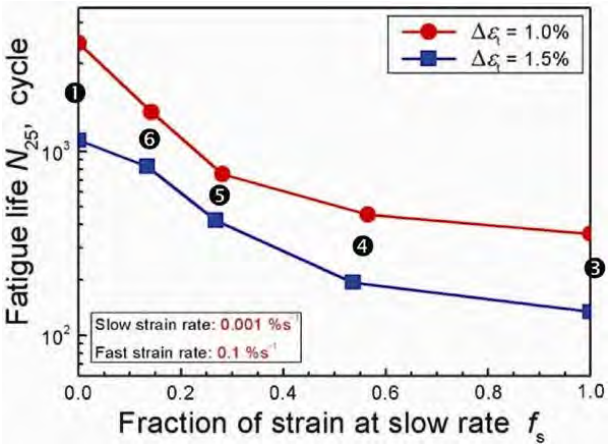

Fig. 6 Effects of fraction of strain at slow rate on fatigue life.

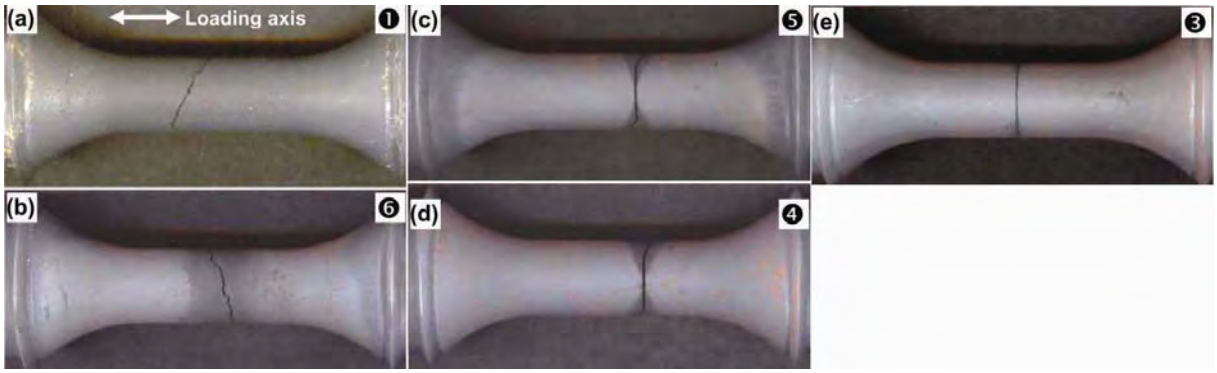

Fig. 7 Influence of strain waveform on fatigue crack morphologies on the specimen surfaces in 561 K 100 ppb water. (a)(b)(c)(d)(e) are corresponding to the strain waveform ❶ ❻ ❺ ❹ ❸ respectively.

3.3 Effects of strain amplitude

The dependence of applied strain amplitude on fatigue life in 561 K air and simulated BWR water for low-alloy RPV steels A508 Cl.3 and A533B (LL-S) are illustrated in Fig. 8 and 9. Under the higher strain amplitude conditions, obvious degradation in fatigue resistance for both of steels was observed in 561 K water relative to 561 K air. This is well consistent with the general viewpoint that LWR environments may degrade the fatigue resistance of pressure vessel steels [2, 5, 7–9]. However, under the low strain amplitude conditions (<0.3 %) or in the high cycle regime (>2×10^4 cycles), both of steels showed relatively better fatigue resistance in 561 K water rather than in 561 K air, contrary to the general viewpoint. There

seemed to exist a critical strain amplitude, above which high temperature water degraded the fatigue resistance of both of steels, while below which the fatigue resistance in high temperature water showed an anomalous enhancement compared to that in high temperature air. In the present study, such a critical strain amplitude was around 0.3 % for both of steels.

The fatigue crack morphologies on specimen surfaces obtained in 561 K air and water were carefully examined. In both air and water, similar crack morphologies were observed for both of steels. Fig. 10 shows a typical example for A508 Cl.3 steel. The fatigue cracks were zigzag with primary orientation about 45^{o} inclined to the loading axis. However, in 561 K water crack branching was frequently observed along the crack path (Fig. 10b), while less crack branching could be found in 561 K air (Fig. 10a). No significant difference in crack morphology could be observed under the different strain amplitude conditions except that less crack branching was found under the low strain amplitudes. The fatigue fractures were similar to the previous observation for A533B (L-S) steel (Fig. 3a to 3d). Namely, featureless fracture surface was observed in 561 K air, on which slight striation-like features remained, while

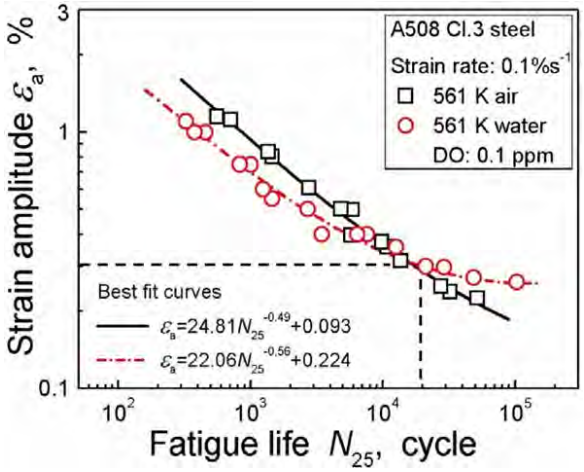

Fig. 8 Dependence of strain amplitude on fatigue life for A508 Cl.3 steel in 561 K air and water.

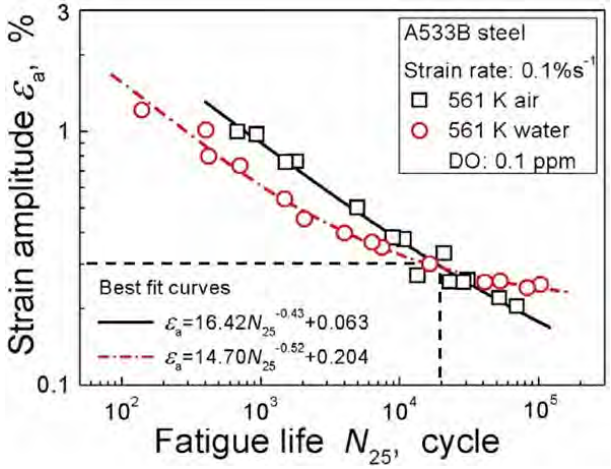

Fig. 9 Dependence of strain amplitude on fatigue life for A533B (LL-S) steel in 561 K air and water.

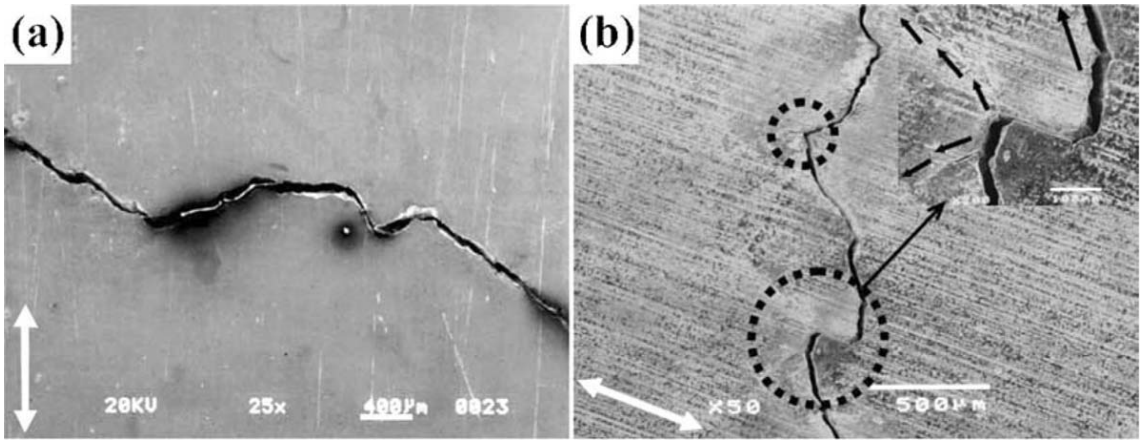

Fig. 10 Fatigue crack morphologies on specimen surfaces of A508 Cl.3 steel in 561 K (a) air and (b) water, 0.4 % strain amplitude and 0.1 %s-1 strain rate.

typical terraced morphologies accompanying secondary cracks were observed on the fracture

surfaces obtained in 561 K water, on which fan-like or quasi-cleavage patterns were frequently found around the sulfide inclusions.

In the present study, a strain-amplitude dependent fatigue resistance appeared in high temperature water. Namely, a better fatigue resistance under the low strain amplitude conditions (<0.3 %) or in the high cycle regime (>2×10^4 cycles) appeared in 561 K water rather than in 561 K air (Fig. 8 and 9), while a distinct degradation in fatigue resistance was observed under the higher strain amplitude conditions in 561 K water. Chopra and Shack's data for A106-Gr B steel in 561 K air and water implied a similar tendency [2]. In the high cycle regime (>10^5 cycles), their best-fit curve for 561 K water was clearly above that for 561 K air. A similar tendency also could be found for A533-Gr B steel if extrapolating their best-fit curves to very high cycle regime (>4 or 5×10^6 cycles). Unfortunately, the exact reason for this strain-amplitude dependent fatigue resistance in high-temperature water environment, especially for the anomalous enhancement in fatigue resistance under the low strain amplitude conditions or in the high cycle regime, is not clear.

The above strain-amplitude dependent fatigue resistance in high temperature water can be partially rationalized if considering the effects of hydrogen-assisted EAC and crack closure. As discussed previously, hydrogen-induced cracking is the dominant EAC mechanism in high temperature water at high strain rate (0.1 $\%s^{-1}$). The applied strain amplitude is believed to affect the above hydrogen-assisted EAC. Under the low strain amplitude conditions, both film-rupture rate at the crack tip and maximum tensile stress ahead of the crack tip are relatively low compared to those under the high strain amplitude conditions. This is unfavorable to the absorption of hydrogen at the crack tip and the transportation of hydrogen into the plastic zone ahead of the crack tip. The hydrogen concentration in the plastic zone thus keeps a lower value compared to the high strain amplitude cases and the hydrogen-assisted brittle cracking effects may be retarded to some extent. Moreover, it should be noted that the present fatigue tests were performed in a total strain control mode. In high temperature water, the hydrogen affected crack-tip metal would have a lower cyclic stress amplitude compared to the hydrogen-free case (in 561 K air) under the same cyclic strain amplitude condition due to the effects of hydrogen-induced softening [10]. This is believed to partially contribute to the better fatigue resistance under the low strain amplitude conditions or in the high cycle regime in 561 K water. Another possible factor may be related to the crack closure induced by corrosion products in high temperature water. The low applied strain amplitude induces a low film-rupture rate at the crack tip under the same strain rate condition. The film (both oxide and other corrosion product films) may reduce the effective stress strength factor range at the crack tip through reducing the crack tip opening displacement, and thus enhance the crack closure, by which the fatigue crack growth rate is reduced. Similar crack closure effects have been reported to play significant roles in the behavior of small cracks or at the stage of near-threshold growth stage [11, 12]. In this regard, the corrosion-product-induced crack closure may partially contribute to the better fatigue resistance under the low strain amplitudes or in the high cycle regime in 561 K water.

4. Conclusions

The effects of loading factors on fatigue resistance and cracking behavior of low-alloy RPV

steels were investigated in simulated BWR water, in which the strain rate, strain waveform and strain amplitude were considered.

It was found that the fatigue resistance and cracking behavior of low-alloy RPV steels were strain-rate dependent in high temperature water. The fatigue life decreased with a decrease in the strain rate, but such a decrease became saturated at the strain rate below a critical value (about 0.001 $\%s^{-1}$ for the present case). At high strain rate, a tortuous cracking morphology was dominant and a rough fracture surface was obtained, on which typical fan-like or quasi-cleavage cracking patterns were frequently observed. An entirely straight cracking morphology, however, became dominant at low strain rate and a flat fracture surface was obtained, on which some evidence of crack arrest was found rather than fan-like or quasi-cleavage cracking patterns. The above strain-rate dependent fatigue cracking behavior may be attributed to a change in dominant EAC mechanism from hydrogen-induced cracking to film-rupture/slip-dissolution-controlled cracking in simulated BWR water.

The applied strain waveforms had obvious effects on the fatigue life of low-alloy RPV steels in simulated BWR water. Increasing the fraction of strain at slow strain rate f_s remarkably decreased the fatigue life, in particular when $f_s < 0.5$, regardless of the applied strain amplitude. The corresponding surface fatigue cracks tended to become entirely straight, which can also be rationalized by the strain-rate dependent EAC mechanism.

A strain-amplitude dependent fatigue resistance was observed for low-alloy RPV steels in simulated BWR water. Under the low strain amplitude conditions (<0.3 %) or in the high cycle regime ($>2\times10^4$ cycles), an enhancement in fatigue resistance was observed for the steels in 561 K water relative to 561 K air, while under the higher strain amplitude conditions, obvious degradation in fatigue resistance was observed in 561 K water. This could be partially attributed to the hydrogen-induced decrease in cyclic stress amplitude and corrosion-product-induced crack closure.

Acknowledgements This study was partially supported by Innovation Fund of IMR, CAS and Fund of Liaoning Province as well as Budget for Nuclear Research of the Ministry of Education, Culture, Sports, Science and Technology in Japan.

References

[1] R. Kilian, A. Roth, *Mater. Corros.* 53 (2002) 727.
[2] O.K. Chopra, W.J. Shack, *Nucl. Eng. Des.* 184 (1) (1998) 49.
[3] H. Hänninen, K. Torronen, M. Kemppainen, S. Salonen, *Corros. Sci.* 23 (6) (1983) 663.
[4] J.D. Atkinson, J. Yu, *Fatigue Fract. Eng. Mater. Struct.* 20 (1) (1997) 1.
[5] O.K. Chopra, W.J. Shack, *J. Press. Vess. Technol. Trans. ASME* 121 (1) (1999) 49.
[6] J.C. Scully, *Corros. Sci.* 20 (8–9) (1980) 997.
[7] M. Higuchi, K. Iida, Y. Asada, *ASTM STP* 1298 (1997) 216.
[8] J . Congleton, E.A. Charles, G. Sui, *Corros. Sci.* 43 (2001) 2265.
[9] O.K. Chopra, W.J . Shack, *ASME PVP* 453 (2003) 71.
[10] X.Q. Wu, I.S. Kim, *Mater. Sci. Eng.* 348A (2003) 309.
[11] A. Saxena, in "*Nonlinear Fracture Mechanics for Engineer*", (CRC Press, New York, 1998), p. 303.
[12] S. Suresh, G.F . Zamiski, R.O. Ritchie, *Metall.Trans.* 12A (1981) 1435.

